Inhibition of Factor Xa by a Peptidyl-α-ketothiazole Involves Two Steps. Evidence for a Stabilizing Conformational Change

Andreas Betz,* Paul W. Wong, and Uma Sinha

Cor Therapeutics, Inc., South San Francisco, California 94080

Received April 27, 1999; Revised Manuscript Received August 2, 1999

ABSTRACT: Recently, peptidylketothiazoles have been shown to be potent inhibitors of proteases, but the details of the interaction have not yet been studied. In the work presented here, the interaction of factor Xa, a coagulation protease, with the transition state inhibitor $BnSO_2$-D-Arg-Gly-Arg-ketothiazole (C921-78) is characterized. C921-78 is a tight and selective inhibitor of the coagulation protease factor Xa (K_d = 14 pM). The hydrolytic activity of factor Xa was inhibited by C921-78 in a time-dependent manner. The rate-limiting step of the bimolecular combination of inhibitor and enzyme was competitive with the substrate. Conversely, the inhibitor could be displaced from the active site of the enzyme after exposure of the preformed complex to an excess of substrate or to the active site inhibitor dansyl-Glu-Gly-Arg-chloromethyl ketone (DEGR-CMK) in a slow reaction. The formation of the C921-78−factor Xa complex resulted in a 60% increase in the magnitude of the fluorescence emission spectrum. Rapid mixing of the enzyme and inhibitor produces a monophasic fluorescence increase, compatible with spectral transition in a single step. The rate constant for this reaction increased hyperbolically with the concentration of C921-78, but the amplitude remained constant. These results are consistent with the initial formation of an enzyme−inhibitor complex (EI), followed by a unimolecular conversion of EI to EI* linked to a spectral transition. The rate constants of the isomerization provide an estimate of 300000-fold stabilization. Thus, the inhibition of factor Xa by C921-78 follows a mechanism similar to that described classically for slow tight binding inhibitors. However, the two steps of the reaction cannot be kinetically separated by the rapid equilibrium assumption, and therefore, the formation of EI is partially rate-limiting, too. The driving energy for the unusually fast isomerization step may result from the highly favorable interactions of the inhibitor in the primary binding site.

Several of the highly specific activation steps of the coagulation cascade are catalyzed by trypsin-like proteases (*3*, *4*). The final product of this activation process, thrombin, promotes the formation of clots by proteolytic conversion of fibrinogen to fibrin and by activation of platelets. Thrombin is the product of the proteolytic cleavage of prothrombin by the prothrombinase complex, which is formed by the association of protease factor Xa and cofactor factor Va on appropriate phospholipid membranes in the presence of calcium ions (*3*−*5*). The cleavage is catalyzed by factor Xa, but its efficiency is markedly enhanced by the accessory components of the prothrombinase complex. The activation of factor X links the intrinsic and extrinsic pathways (*6*). Because of this central role of factor Xa in the coagulation pathway, the modulation of factor Xa activity is an attractive approach for the regulation of hemostasis (*7*).

Although several macromolecular inhibitors of factor Xa have been described (*8*, *9*), there has recently been considerable interest in the development of low-molecular weight inhibitors. Because of the low abundance of factor Xa, a potential inhibitor requires a low dissociation constant and high selectivity. As all coagulation proteases have a preference for ligands with arginine in their reactive centers, the selectivity of small inhibitors for factor Xa must be enhanced by using the preferences of the enzyme at secondary binding sites. On the basis of the sequence D-Arg-Gly-Arg of a highly selective and efficient substrate of factor Xa, inhibitors of factor Xa were designed by replacing the scissile bond of the substrate with a carbonyl group with an activating substituent (*10*). Heterocyclic substituents were preferred since they have recently been used successfully to synthesize highly potent inhibitors of thrombin and elastase. In X-ray structures of the complexes of these inhibitors with protease, the interaction of the electrophilic carbonyl C atom with the nucleophilic serine 195[1] of the charge relay system stabilizes the protease−inhibitor complex via formation of a hemiketal bond in a transition state. In addition, a hydrogen bond forms between His57 and the nitrogen atom of the heterocycle (*11*, *12*). The resulting complex closely emulates the transition state of hydrolysis of peptide substrates, where after formation of the covalent bond between Ser195 and the scissile carbonyl, the amide nitrogen abstracts a proton from the protonated His57 (*12*). The participation of His57 in the binding of the inhibitors has until recently been reported only for mechanism-based irreversible inhibitors (*1*, *13*). Thus,

* To whom correspondence should be addressed: Cor Therapeutics, Inc., 256 E. Grand Ave., South San Francisco, CA 94080. Phone: (650) 246-7301. Fax: (650) 244-9270. E-mail: abetz@corr.com.

[1] The amino acid numbering is based on the numbering for chymotrypsin following the convention of Bode et al. (*1*).

10.1021/bi990958a CCC: $18.00
Published on Web 10/08/1999

the peptide α-ketoheterocycles represent the first group of stable mechanism-based, fully reversible inhibitors.

Many transition state inhibitors combine slowly with proteases, but the basis for this behavior remains controversial (*14*−*16*). Rate-limiting conformational changes in the enzyme−inhibitor complex were inferred to cause slow binding in the inhibition of thrombin and elastase (*17*, *18*). In contrast, the X-ray structures of complexes of proteases with slow inhibitors indicate no structural difference between the free and the inhibitor-bound enzyme, but support a "lock and key" mechanism (*15*, *19*). In addition, the slow interconversion between different forms of inhibitor and enzyme has been found to result in a slow onset of the inhibition (*15*, *16*). Similar detailed kinetic studies have not been conducted for the binding of small transition state inhibitors of factor Xa.

In the work presented here, the mechanism of the inhibition of human factor Xa and $BnSO_2$-D-Arg-Gly-Arg-ketothiazole (structure **1**) was investigated by steady state kinetics and stopped flow methods.

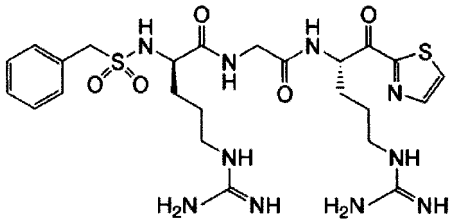

(1)

C921-78 was shown to be a tight and relatively selective inhibitor, which forms a complex with factor Xa via a two-step mechanism. One step was characterized by a change in intrinsic fluorescence of factor Xa, which indicates a conformational change in the protease−inhibitor complex.

EXPERIMENTAL PROCEDURES

Reagents and Proteins. Hepes, chromozym TH (tosyl-glycyl-prolyl-arginyl-*p*-nitroanilide), and chromozym PL (tosyl-glycyl-prolyl-lysyl-*p*-nitroanilide) were from Roche. PEG 8000[2] was from J. T. Baker (Philippsburg, NJ). L-α-Phosphatidylcholine (PC) and L-α-phosphatidylserine (PS) were obtained from Avanti Polar Lipids (Alabaster, AL) and Sigma (St. Louis, MO). Dansyl-glutamyl-glycyl-arginyl-chloromethyl ketone (DEGR-CMK) was from Calbiochem (La Jolla, CA). The inhibitor DEGR-CMK was dissolved in 10 mM HCl to a 90 mM stock (E_{330} = 3500 M^{-1} cm^{-1}). The inhibitor C921-78 (benzenesulfonyl-D-arginyl-glycyl-arginyl-α-ketothiazole) was dissolved in water, and the concentrations of stock solutions of the inhibitor were determined spectrophotometrically (E_{293} = 20.8 M^{-1} cm^{-1}). The substrate Spectrozyme Xa (methoxycarbonyl-glycyl-glycyl-arginyl-*p*-nitroanilide) (SpXa) and Spectrozyme PCa [H-D-lysyl(γ-carbobenzoxy)prolyl-arginyl-*p*-nitroanilide] were obtained from American Diagnostica (Greenwich, NY). S-2765 (carbobenzoxy-D-arginyl-glycyl-arginyl-*p*-nitroanilide) was from Diapharma (West Chester, OH). The substrates were dissolved in water, and the concentrations were determined spectrophotometrically in 20 mM Hepes and 0.15 M NaCl (pH 7.4) (E_{342} = 8270 M^{-1} cm^{-1}) (*20*). Vesicles (PCPS) were prepared by size exclusion filtration of an emulsion of 75% L-α-phosphatidylcholine and 25% L-α-phosphatidylserine (*21*). The concentrations of phospholipids were determined using a colorimetric assay for inorganic phosphate (*22*). Trypsin was obtained from Worthington (Lakewood, NJ) and repurified on a benzamidine column. The proteins human factor Xa, factor Va, thrombin, and plasmin were purchased from Haematologic Technologies (Essex Junction, VT). The purity of factor Xa was assessed by SDS−PAGE on reducing and nonreducing gels. The protein concentrations were determined using the following molecular weights and extinction coefficients ($\epsilon_{280}^{0.1\%}$): factor Va, 168 000 and 1.74 (*23*); factor Xa, 45 300 and 1.16 (*24*); thrombin, 37 500 and 1.53 (*25*); plasmin, 70 000 and 1.68 (*26*); and trypsin, 23 800 and 1.53 (*26*).

Table 1: Dissociation Constants of C921-78 with Various Proteases[a]

enzyme	inhibition constant (nM)	enzyme	inhibition constant (nM)
factor Xa	0.014[b]	activated protein C	2900[c]
thrombin	1600[c]	trypsin	0.5[b]
plasmin	336[c]		

[a] The dissociation constants were determined as described in Experimental Procedures for the different types of inhibitors. [b] Determined from the analysis of titration curves using eqs 1 and 2. [c] Determined assuming complete competitive inhibition. The substrates and the concentrations for the individual enzymes were as follows: trypsin, 0.5 nM trypsin with chromozym TH; IIa, 1 nM thrombin with chromozym TH; plasmin, 5 nM plasmin with chromozym PL; and protein C, 8 nM protein C with Spectrozyme PCa.

All assays were preformed in 20 mM Hepes, 150 mM NaCl, 10 mM $CaCl_2$, and 0.1% PEG 8000 (pH 7.4) (assay buffer). When the concentration of the enzyme was less than 0.5 nM, the reaction vessels were pretreated with 0.02% Tween 80, 20 mM Hepes, and 150 mM NaCl (pH 7.4) for 2 h at room temperature and then dried by centrifugation.

Steady State Measurements. For the determination of the dissociation constant of C921-78 with factor Xa, increasing concentrations of inhibitor were incubated with 0.1 and 0.2 nM factor Xa for 2 h in a total volume of 150 μL. For the determination of the residual enzyme activity, 50 μL of 800 μM SpXa in buffer was added. After mixing, the initial rates were monitored for 5 min in a V_{max} plate reader (Molecular Devices, Menlo Park, CA). Since negligible dissociation of the complex during this period was assumed, the concentrations used in the calculations correspond to those before addition of substrate. The dissociation constant of C921-78 with trypsin was determined from the steady state rate of hydrolysis of chromozym TH in the presence of the inhibitor.

The dissociation constant of C921-78 with plasmin, activated protein C, and thrombin was determined by adding the enzyme to mixtures with increasing substrate concentrations at different fixed inhibitor concentrations. Hydrolysis was initiated by addition of enzyme to the final concentration as indicated in Table 1. The initial rates of substrate

[2] Abbreviations: DEGR-CMK, dansyl-glutamyl-glycyl-arginyl-chloromethyl ketone; EGR-CMK, glutamyl-glycyl-arginyl-chloromethyl ketone; EGR-factor Xa, factor Xa inactivated with EGR-CMK; PCPS, small unilamellar vesicles composed of 25% (w/w) L-α-phosphatidylserine and 75% L-α-phosphatidylcholine; HPLC, high-performance liquid chromatography; PEG 8000, polyethylene glycol with an average molecular weight of 8000; S-2765, carbobenzoxy-arginyl-glycyl-arginyl-*p*-nitroanilide; SpXa, methoxycarbonyl-glycyl-glycyl-arginyl-*p*-nitroanilide.

hydrolysis were measured by monitoring the absorbance at 405 nm using a V_{max} kinetic plate reader.

Determination of the Association Rate Constant. Reaction mixtures (150 μL) of 266 μM SpXa with increasing concentrations of inhibitor were prepared in coated microplate assay plates. Reactions were initiated by addition of 50 μL of a 200 nM solution of factor Xa in assay buffer. Hydrolysis of SpXa was followed continuously in a V_{max} kinetic microplate reader at ambient temperature over a 2 h period. The stability of the enzyme in this time period was established by the test developed by Selwyn (*27*).

Determination of the Dissociation Rate Constant. The enzyme−inhibitor complex was preformed by incubating 50 nM factor Xa and 75 nM C921-78 in assay buffer, and complete inhibition of factor Xa activity was confirmed by chromogenic assay. The time-dependent increase in enzymatic activity was measured following dilution of an aliquot (5 μL) into 1 mL of 1 mM S-2765 in a Tween 20-coated cuvette for 4 h.

Displacement of C921-78 by DEGR-CMK from Factor Xa. After incubation of 4 μM factor Xa and 6 μM C921-78 in 50 mM Tris, 150 mM NaCl, and 2 mM $CaCl_2$ (pH 7.4), complete formation of the enzyme−inhibitor complex was confirmed by chromogenic assay. To a preformed enzyme−inhibitor complex was added a concentrated stock solution of DEGR-CMK to a final concentration of 1 mM. After timed intervals, 80 μL aliquots were removed from the reaction mixture and the reactions therein quenched by addition of 120 μL of glacial acetic acid. The samples were dialyzed overnight in 0.5 M concentrated acetic acid and evaporated to dryness. Detection and quantitation of the formed DEGR−factor Xa complex were accomplished by reducing SDS−PAGE and HPLC analysis. Following electrophoresis, the fluorescent bands were visualized by UV illumination and the protein bands by staining with Coomasie brillant blue R-250. For the HPLC method, the samples were dissolved in 50% acetic acid and loaded on a 25 cm Vydac C-4 (214TP54) column. The protein was eluted with a gradient linearly increasing from buffer A (0.1% TFA) to 60% buffer B (75% acetonitrile and 0.1% TFA) over the course of 40 min with a flow rate of 0.75 mL/min. Factor Xa was detected by absorbance (280 nm) and fluorescence (λ_{ex} = 280 nm, λ_{em} = 520 nm with a bandwidth of 20 nm). The fraction of factor Xa containing covalently linked inhibitor was determined from the ratio of the integrated areas under the absorbance and fluorescence peaks (*28*).

Steady State Fluorescence Measurements. Fluorescence measurements were performed in 3 mL quartz cuvettes at room temperature using an SLM Aminco Series 2 fluorometer. The fluorescence was recorded at 278 (excitation) and 320 (emission) following incremental addition of C921-78 (2 μL) to 100 nM factor Xa or active site-blocked EGR-factor Xa and mixed by aspiration with a pipet.

Stopped Flow Measurements of Factor Xa Inhibition. The increase in fluorescence after rapid mixing of equal volumes of C921-78 and factor Xa solutions was followed in an RSM1000 stopped flow spectrofluorometer (Olis Instruments, Bogart, GA). The final concentrations of the reactants were half of those present in the driving syringes. The experiments were performed under pseudo-first-order conditions ($I \geq 5E$). To compensate for the considerable inner filter effect at high inhibitor concentrations, the enzyme concentration was adjusted appropriately to increase the signal-to-noise ratio. The fluorescence signal was collected over at least five to ten half-life times. Average rate constants were derived from five to ten replicate traces.

Data Analysis. Data were analyzed using the indicated equations by nonlinear regression using the Marquardt algorithm (*29*). The fitted data are presented with 95% confidence levels.

Inhibition of Plasmin, Thrombin, and Activated Protein C by C921-78. From intial velocity data obtained with plasmin, thrombin, and activated protein C, K_i, K_m, and V_{max} were determined using the equation for simple, complete competitive inhibition (*30*).

Inhibition of Factor Xa and Prothrombinase by C921-78. Residual enzyme activities obtained after incubation of increasing concentrations of C921-78 with two fixed enzyme concentrations were analyzed using eqs 1 and 2:

$$E_i = \frac{nI + E + K_d^* - \sqrt{(nI + E + K_d^*)^2 - 4nIE}}{2} \quad (1)$$

$$v_{obs} = v_\infty E + v_o E\left(1 - \frac{E_i}{E}\right) \quad (2)$$

where E and I are the total concentrations of the enzyme and inhibitor, respectively, E_i is the concentration of the inhibited enzyme, K_d^* is the overall dissociation constant, v_o and v_∞ represent the initial rates of substrate hydrolysis at zero and infinite inhibitor concentrations, respectively, and n is the number of moles of inhibitor bound per mole of enzyme at saturation.

Kinetics of Enzyme Inhibition of Factor Xa by C921-78. The second-order rate constant of the reaction of C921-78 with factor Xa was obtained by progress analysis. The progress curves of substrate hydrolysis by factor Xa in the presence of inhibitor were analyzed by nonlinear regression using the equation (*31*, *32*)

$$P = v_s t + \frac{(v_o - v_s)}{k_{obs}}(1 - e^{-k_{obs}t}) + \text{offset} \quad (3)$$

where P represents the absorbance at 405 nm at any time t, v_o and v_s are the rates before and after the onset of inhibition, respectively, and k_{obs} is the rate of the transition from v_o to v_s. For analysis, the resulting progress curves were corrected for the delay between the start of the reaction and the onset of the absorbance measurements in seconds. The obtained rate constants were analyzed using eq 4 to obtain an estimate of k_{inh}. Because of the small inhibitor concentrations that were used, the equation contains a term for the reduction of the total inhibitor concentration by formation of the enzyme−inhibitor complex (called I_{eff}) (*33*)

$$k_{obs} = k_{inh}\sqrt{(K_d^* + E + I)^2 - 4IE} \quad (4)$$

where K_d is the dissociation constant of the enzyme−inhibitor complex and E and I are the total concentrations of enzyme and inhibitor, respectively. If substrate and inhibitor bind competitively to the active site of factor Xa, the value of k_{inh} will depend on the substrate concentration represented by eq 5 (*34*, *35*)

$$k_{inh}' = \frac{k_{inh}K_m}{K_m + S} \quad (5)$$

where S is the substrate concentration and K_m the Michaelis constant of SpXa with factor Xa. The Michaelis constant for the hydrolysis of SpXa by human factor Xa was determined from initial rate measurements.

Determination of the Dissociation Rate Constant. The exponential recovery of hydrolytic activity was continuously monitored by the absorbance, after the preformed factor Xa−C921-78 complex was diluted into an excess of 1 mM S-2765 to a final concentration of 0.3 nM. The resulting progress curve was analyzed using eq 6 (*32*):

$$P = v_o t + v_s \frac{(e^{-k_{off}t} - 1)}{k_{off}} \quad (6)$$

where P is the absorbance at 405 nm, v_s the steady state rate, k_{off} the off rate constant, and v_o the initial rate of substrate hydrolysis. When the dissociation of the inhibitor−factor Xa complex was followed by reaction of the free factor Xa with the fluorescence active site label DEGR-CMK, the dissociation rate constant was determined from eq 7:

$$F_{obs} = F_o + (F_o - F_\infty)e^{-k_{off}t} \quad (7)$$

where F_{obs} represents in this case the area under the fluorescence signal corrected for the area of the signal at 280 nm (the amount of protein). F_∞ is the fluorescence reached at infinite reaction time and was obtained by reacting free factor Xa with DEGR for 1 h. k_{off} was obtained by nonlinear regression.

Fluorescence Measurement of the Binding of C921-78 to Factor Xa. The increase in fluorescence resulting from the addition of C921-78 to a solution of factor Xa was analyzed using eq 8:

$$F_{corr} = F_o + \Delta F \frac{EI}{E} \quad (8)$$

where F_{corr} is the observed fluorescence after correction for the inner filter effect of the inhibitor, F_o the fluorescence in the absence of the inhibitor, and ΔF the increase in fluorescence at infinite inhibitor concentrations. The term EI was calculated with eq 1.

Data Analysis of Stopped Flow Measurements. The increase in fluorescence induced by rapid mixing of C921-78 and factor Xa was analyzed by nonlinear regression using

$$F_t = \text{offset} + Q(1 - e^{-k_{obs}t}) \quad (9)$$

where F is the fluorescence signal at time t, k_{obs} the pseudo-first-order rate constant, Q the amplitude of the fluorescence increase, and t the time.

The time-resolved fluorescence spectra of the reaction of C921-78 and factor Xa were collected into a matrix with an $m \times n$ format. The data were analyzed by singular-value decomposition (SVD) and exponential fitting by a Simplex algorithm using the Olis Global Fitting Program (*36*) The procedure generates two matrixes **V** and **US**. The eigenvectors of **V** represent the basis spectra of the different species in the reaction mixture. The matrix **US** contains the rate constants and the time evolution of each species, represented by the eigenvector amplitude normalized to unity. The methods permit the sensitive detection of intermediates and the determination of the rate constants of their decays.

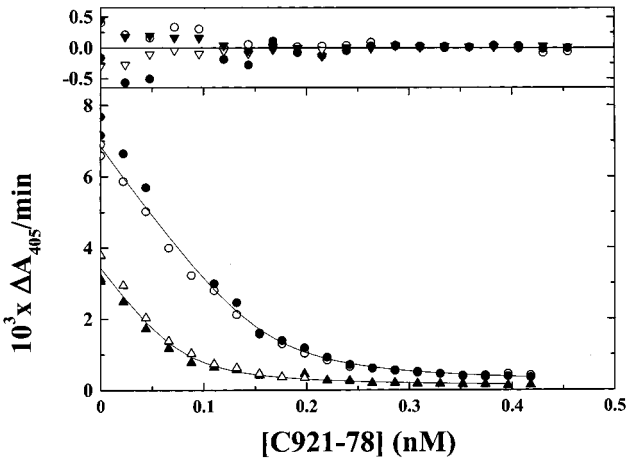

FIGURE 1: Inhibition of factor Xa by C921-78. Residual factor Xa activity was measured using SpXa after a 2 h incubation of mixtures containing 0.2 nM (○ and ●) or 0.1 nM factor Xa (△ and ▲) and the indicated concentration of inhibitor. The lines were drawn after nonlinear regression analysis with eqs 1 and 2, which yields the following parameters: $v_o = (35.6 \pm 0.6) \times 10^{-3}$ A_{405} min^{-1} (nM factor Xa)$^{-1}$, $v_\infty = (0.43 \pm 0.44) \times 10^{-3}$ A_{405} min^{-1} (nM factor Xa)$^{-1}$, $n = 1.31 \pm 0.05$ mol of C921-78/mol of factor Xa, and $K_d^* = 14.1 \pm 3$ pM. The residuals for the fitted lines are illustrated in the upper panel.

RESULTS

Selectivity of C921-78 for Factor Xa. Preliminary experiments demonstrated a high affinity of factor Xa for C921-78, and substrate hydrolysis was significantly inhibited at equal concentrations of enzyme and inhibitor. Thus, analysis of this interaction in terms of classical inhibition was no longer appropriate, and the dissociation constant of the factor Xa−C921-78 complex was determined by titration of the protease with the inhibitor (Figure 1). The concentration of the remaining free enzyme was estimated from the residual hydrolytic activity following addition of substrate. Since the rate of substrate hydrolysis remained constant over the observation period, no inhibitor was displaced from the complex. Analysis of the data yielded a surprisingly low dissociation constant of C921-78 with factor Xa ($K_d = 14$ pM). The stoichiometry of 1.25 mol of inhibitor/mol of factor Xa excludes inhibition by a contaminant remaining from the synthesis of C921-78. The very low dissociation constant of the CT50034 factor Xa was confirmed in a comparable experiment at a concentration of 20 pM protease, which yielded a K_d of 30 pM (data not shown). The deviation of the stoichiometry from unity may result from an underestimation of the extinction coefficient of factor Xa and has also been observed in active site titrations of factor Xa. In a separate experiment, factor Xa was incubated with C921-78 in the presence of saturating concentrations of phospholipids and factor Va. The analysis of the inhibition data yields an almost identical dissociation constant (22 ± 4 pM), indicating no significant influence of the cofactor on the enzyme−inhibitor interaction.

The reaction of C921-78 with trypsin yielded weaker inhibitory complexes, and the addition of substrate in titration experiments resulted in rapid dissociation of the complex.

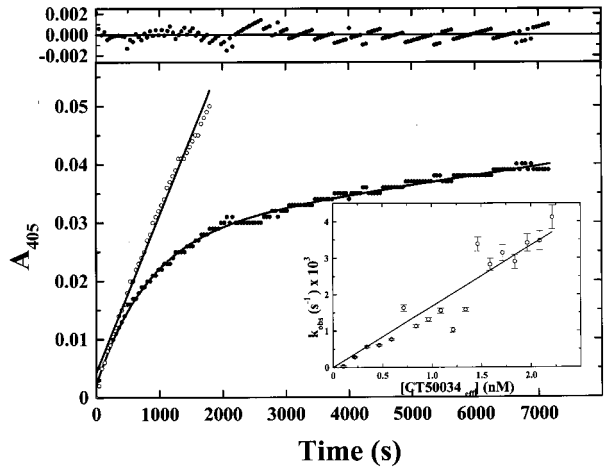

FIGURE 2: Kinetics of the inhibition of factor Xa by C921-78. The reactions, mixtures containing 200 μM SpXa in assay buffer without (○) or with 1.3 nM C921-78 (●), were initiated by addition of 50 pM factor Xa. Product formation was monitored at room temperature and analyzed as described in Data Analysis. The line was drawn according to eq 3, using the following fitted parameters: $k_{obs} = (1.208 \pm 0.01) \times 10^{-3}$ s^{-1}, $v_o = (3.4 \pm 0.4) \times 10^{-5}$ OD/min, $v_s = (1.64 \pm 0.021) \times 10^{-6}$ OD/min, and the offset $= (7.7 \pm 1.4) \times 10^{-3}$ OD/min. The inset shows the dependence of the rate of the reaction of C921-78 with factor Xa on the effective concentration of inhibitor under first-order conditions. The individual rate constants were determined under the conditions described above. The pseudo-first-order rate constant for the individual reaction and the effective inhibitor concentration were calculated using eqs 3 and 4, respectively. Weighted nonlinear regression of the data yields the observed rate constant of inhibition at a substrate concentration of 200 μM SpXa [$k_{inh}' = (1.63 \pm 0.07) \times 10^6$ M^{-1} s^{-1}].

Thus, the dissociation constant was determined from the steady state rate reached after the enzyme had been added to a mixture of substrate and inhibitor. Surprisingly, the affinity of C921-78 for trypsin is only 30-fold lower than that for factor Xa ($K_d = 0.5$ nM).

In contrast to those of factor Xa, relatively high concentrations of C921-78 are required to significantly inhibit the related proteases plasmin, thrombin, and activated protein C. Analysis of the data using the rate expression for classical competitive inhibition yielded dissociation constants of C921-78 with activated protein C, thrombin, and plasmin which were several thousand times higher than those for factor Xa (Table 1). Thus, C921-78 exhibits a strong preference for factor Xa and trypsin. When compared to the data for selected coagulation proteases, these data suggested a high selectivity of C921-78 for factor Xa.

Rate of Reaction of C921-78 with Factor Xa. To further characterize the interaction of C921-78 with factor Xa, substrate hydrolysis by factor Xa was continuously monitored in the presence of inhibitor (Figure 2). The progress curves of substrate hydrolysis showed an exponential decline in hydrolytic activity until a steady state was reached. With the inhibitor concentration being much greater than the concentration of the enzyme, progress curves were analyzed according to eq 3 to yield the pseudo-first-order rate constant of the reaction. A linear increase in a pseudo-first-order rate constant with the inhibitor concentration indicates that a bimolecular reaction is the slow step of complex formation. From the slope (Figure 2, inset), the association rate constant at a certain substrate concentration of enzyme and inhibitor

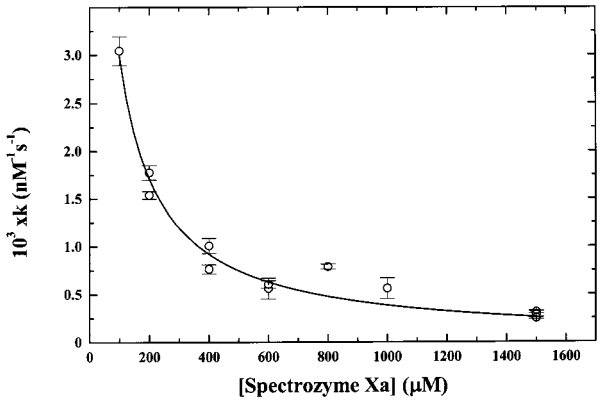

FIGURE 3: Effect of substrate on the rate of factor Xa inhibition by C921-78. The apparent inhibition rate constants were determined at the indicated concentrations of SpXa. The assays were performed and the data analyzed as described in the legend of Figure 2. A plot of the apparent inhibition rate constants vs the pertinent substrate concentrations was analyzed by nonlinear regression using eq 5. The drawn line represents the best fit using a K_m of 33 $\pm$ 15 μM and a substrate-independent inhibition rate constant k_{inh} of 0.012 $\pm$ 0.0045 nM^{-1} s^{-1}.

was determined, following correction for inhibitor bound to factor Xa (I_{eff}). From the data, a rate of association was determined to be $(1.63 \pm 0.07) \times 10^6$ M^{-1} s^{-1} at a SpXa concentration of 200 μM. As a consequence of the small steady state rates determined from the progress curve, the ordinate intercept was too small for deriving an exact estimate for the dissociation rate constant.

The effect of substrate on the rate of inhibition of factor Xa by C921-78 is illustrated in Figure 3. The rate of inhibition declines hyperbolically with increasing SpXa concentration. If steady state conditions are assumed for the interaction of the substrate and factor Xa, the inhibition rate constant should only depend on terms for K_m and the concentration of the substrate. Nonlinear regression using eq 5 yields values of 1.2×10^7 M^{-1} s^{-1} for the inhibition rate constant and a K_m of 33 $\pm$ 13 μM for SpXa used as the substrate, a value close to that determined independently by the initial rates of substrate hydrolysis. Thus, the rate-limiting step of complex formation involves the site interacting with the substrate. Similar results were also obtained with another factor Xa substrate, S-2765 (data not shown).

Dissociation Rate Constant of the C921-78−Factor Xa Complex. The fast and tight binding of C921-78 to factor Xa prevents an exact determination of the dissociation rate constant from progress curves. The dissociation rate constant was inferred from the recovery of enzymatic activity after the preformed enzyme inhibitor complex was diluted 100-fold into assay buffer containing an excess of substrate, which significantly reduces the rate of reassociation of factor Xa with the inhibitor. A steady state for the reaction was reached after 90 min ($t_{1/2} = 23$ min). A single-exponential fit to eq 7 yields a dissociation rate constant of $(5.43 \pm 0.023) \times 10^4$ s^{-1}. In accord with a general competitive mechanism, the data demonstrate that inhibition of factor Xa by C921-78 is substantially reversed upon dilution at high substrate concentrations. However, even after dilution, the concentration of C921-78 still exceeded the apparent dissociation constant by 50-fold; this method overestimates the dissociation rate constant, and full activity is not recovered.

Scheme 1

$$E + I \underset{k_{off}}{\overset{k_{on}}{\rightleftharpoons}} EI \qquad K_d = k_{off}/k_{on}$$

For additional characterization, the time-dependent displacement of C921-78 from the active site of factor Xa by DEGR-CMK was investigated. DEGR-CMK forms an irreversible fluorescent complex by covalent modification of His57 and Ser195 in the catalytic triad of factor Xa (*28*, *37*), and this precludes reassociation of C921-78 with the protease. Because of the large excess of DEGR-CMK, only the dissociation of the C921-78−factor Xa complex should be rate-limiting. As described in Experimental Procedures, the time course of the formation of the fluorescent adduct of factor Xa and DEGR-CMK was followed by HPLC analysis of samples withdrawn from an ongoing reaction. A dissociation rate constant (k_{off}) was determined by monitoring the time course of 50% conversion of the C921-78−factor Xa complex to DEGR-factor Xa to be (1.72 ± 0.03) × 10^{-5} s^{-1}. Because of the long observation period, significant decay of DEGR-CMK and inactivating autolysis of factor Xa cannot be excluded, and the resulting rate probably represents an underestimate of the dissociation rate constant. Moreover, to confirm the covalent modification of factor Xa by DEGR-CMK, the reaction was also followed by gel electrophoresis. Qualitatively, this demonstrates that dissociation of the inhibitor occurs with release of active factor Xa without detectable chemical modification of active site residues.

The following scheme (Scheme 1) summarizes the kinetic results of the reaction of factor Xa with C921-78 obtained under steady conditions in the presence of substrate.

In conclusion, the results of these steady state studies on the inhibition of factor Xa by C921-78 can be represented by a one-step mechanism. However, substitution of the values for the association rate and dissociation rate constants into Scheme 1 yields a K_d of 123 pM. This discrepancy in the values for the dissociation constant obtained from kinetic measurements and titration indicates that Scheme 1 does not account for all steps in the reaction of C921-78 with factor Xa. Thus, the reaction was further investigated by more rigorous methods.

Equilibrium Fluorescence Titration of Factor Xa by C921-78. Previous studies found significant changes in the intrinsic fluorescence of serine proteases resulting from the binding of inhibitors to the active site (*38*). Similarly, the incremental addition of C921-78 to a solution of factor Xa produced a saturable increase in the relative fluorescence to a maximum value of 60% (Figure 5). Since in the experiment the concentration of C921-78 that was used was much higher than the dissociation constant determined previously, a sharp break was obtained in the titration curve at the equivalence point, indicating formation of a bimolecular complex. The subsequent independence of the fluorescence on the concentration of C921-78 is an indication of the insignificant contribution of C921-78 to the fluorescence of the solution. Analysis of the titration curve yielded a stoichiometry of 1.2 which is identical to that obtained in the determination of the dissociation constant of the C921-78−factor Xa complex using activity measurements (Figure 1). In contrast, the titration of factor Xa with the active site covalently blocked

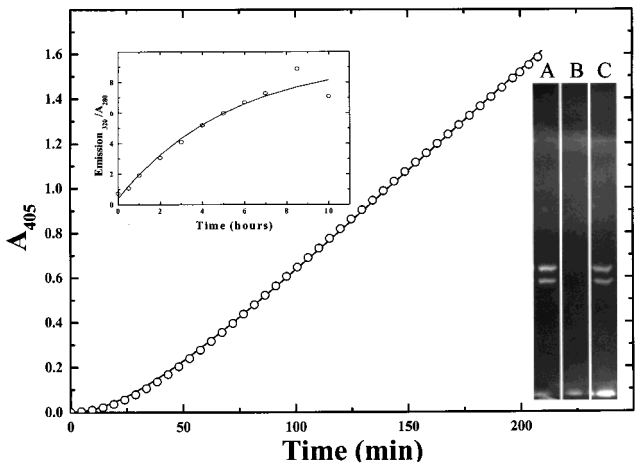

FIGURE 4: Dissociation of the C921-78−factor Xa complex. The dissociation of the preformed C921-78−factor Xa complex in the presence of substrate was monitored by the recovery of hydrolytic activity. The final concentrations of reactants were 0.25 nM factor Xa, 0.375 nM C921-78, and 1 mM S-2765. The progress curve of substrate hydrolysis was analyzed using eq 6 to yield a k_{off} of (5.43 ± 0.023) × 10^{-4} s^{-1} and a v_s of (1.423 ± 0.002) × 10^{-4} mOD/s. Inset A shows the displacement of C921-78 from factor Xa by DEGR-CMK. The preformed C921-78−factor Xa complex was diluted into 1 mM DEGR-CMK in 100 mM Tris and 150 mM NaCl. Reactions were quenched by addition of acetic acid to a concentration of 50% at the indicated time points. The line was drawn after nonlinear regression using eq 7 with the following parameters: k_{off} = (5.2 ± 0.6) × 10^{-5} s^{-1}, F_∞ = 9.56 ± 1.3, and F_o = 0.387 ± 0.43. Inset B shows the gel of significant time points in the reaction of factor Xa with DEGR-CMK in the absence and presence of C921-78. The experiment was performed as described in Experimental Procedures. After electrophoresis, the protein bands were visualized in UV light. The lanes are labeled as follows: A, factor Xa without C921-78 reacted with DEGR-CMK (incubation for 0 min); B, factor Xa with C921-78 reacted with DEGR-CMK (incubation for 0 min); and C, factor Xa with C921-78 reacted with DEGR-CMK (incubation for 5 h).

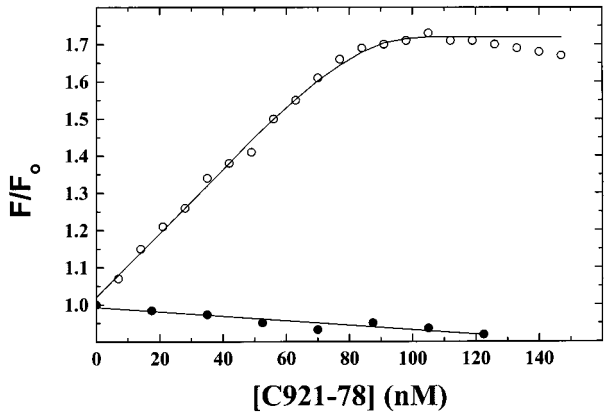

FIGURE 5: Fluorescence titration of factor Xa with C921-78. Reaction mixtures containing 100 nM factor Xa in 20 mM Hepes and 150 mM NaCl (pH 7.4) were titrated with increasing concentrations of inhibitor at 25 °C. Upon addition of incremental amounts of C921-78 to factor Xa (○) and EGR-factor Xa (●), the relative fluorescence change at 278 nm (λ_{ex}) and 320 nm (λ_{em}) was monitored The line was drawn according to eq 8 using the following fitted constants: K_d = 0.30 ± 0.22 nM, $\Delta F_\infty/F_o$ = 0.76 ± 0.011, F_o = 1.025 ± 0.007, and stoichiometry n = 1.212 ± 0.018.

EGR-CMK produced no comparable change in the intrinsic fluorescence. This observation is consistent with the assumption of binding of C921-78 exclusively to the active site of factor Xa. In addition, this experiment demonstrates also the

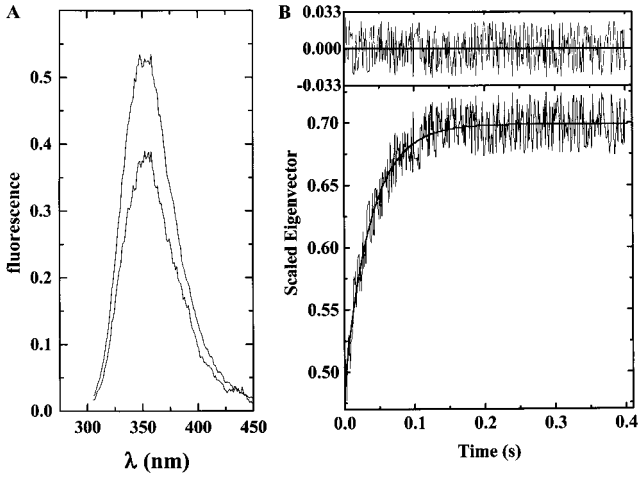

FIGURE 6: Analysis of time-resolved spectra of the reaction of C921-78 with factor Xa. The fluorescence changes induced by the reaction of 5 μM C921-78 with 1 μM factor Xa in assay buffer. The emission spectra were recorded with 1000 scans/s. (A) SVD was used to extract the spectral components from the time-resolved emission spectrum of the reaction. (B) Time course of the amplitude of the calculated product spectrum of the reaction of C921-78 with factor Xa. The scaled eigenvector represents the relative amplitude of the product spectrum at each time point, normalized to unity. The line represents the result of a nonlinear regression using eq 9 with the following parameters: $k_{obs} = 26 \pm 0.94$ s^{-1}, $Q = 0.209 \pm 0.004$, and offset $= 0.489 \pm 0.005$.

absence of significant inner filter effects, which resulted in an only 5% decrease in the intrinsic fluorescence at the maximal C921-78 concentration. Thus, changes in the intrinsic fluorescence can be used to follow the formation of the C921-78−factor Xa complex.

Fluorescence Stopped Flow Studies of the Binding of C921-78 to Factor Xa. The conventional determination of the rate constants of the inhibition of factor Xa from progress curves of substrate hydrolysis is limited by the detection limits of the resulting signal and by potential artifacts introduced by the kinetics of the reaction of the enzyme and substrate. Therefore, the kinetics of factor Xa binding to C921-78 were monitored by the intrinsic fluorescence change of the protease upon rapid mixing by stopped flow techniques. To detect transient fluorescence changes, time-resolved emission spectra in the course of the reaction of enzyme and inhibitor were monitored in the interval from 320 to 450 nm (Figure 6A) using a stopped flow spectrofluorometer. The resulting set of spectra was analyzed by singular-value decomposition, which makes it possible to determine the spectra and evolution of intermediates during a reaction. Analysis of the wavelength component of the emission spectra yielded two basis components, indicating only a single optical transition upon binding of the inhibitor to factor Xa. The resulting spectra are qualitatively consistent with the increase in the fluorescence intensity observed in the titration of factor Xa by C921-78. The time course of the spectral change is represented by the calculated eigenvector, resulting from the time-dependent changes in the amplitude at the various wavelengths of the emission spectra (Figure 6B). During the reaction, the fluorescence intensity increased by 50% in a single-exponential manner. This fluorescence enhancement corresponds approximately to the difference in the amplitudes of free factor Xa and the enzyme−inhibitor complex. Accordingly, the change in

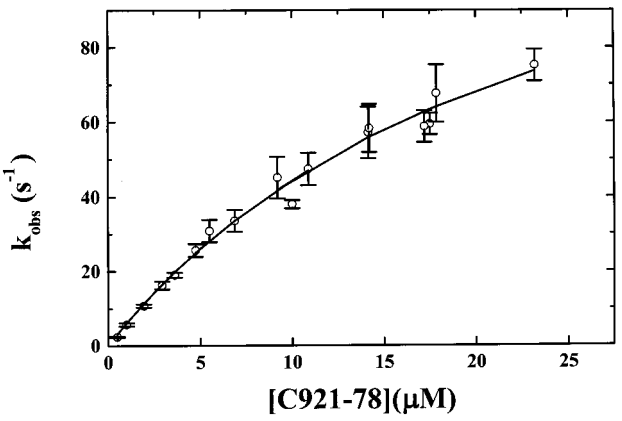

FIGURE 7: Dependence of k_{obs} on the concentration of C921-78. Stopped flow measurements were conducted at the indicated inhibitor concentrations under pseudo-first-order conditions with varying enzyme concentrations. The resulting data were analyzed using eq 9, and the error indicates the deviation from the average of at least six determinations. The line results from a fit of the values to a rectangular hyperbola with a limiting rate of 147 ± 15 s^{-1} and a midpoint $K_{0.5}$ of 23 ± 3.7 μM. The values were interpreted in terms of Scheme 2.

Scheme 2

$$E + I \underset{k_2}{\overset{k_1}{\rightleftharpoons}} EI \underset{k_4}{\overset{k_3}{\rightleftharpoons}} EI^*$$

fluorescence intensity after mixing of the enzyme and inhibitor occurs in one step without detectable intermediates with different optical properties.

To investigate the mechanism of the reaction of C921-78 with factor Xa, the dependence of the observed rate constant on the inhibitor concentration was examined. In these reactions, pseudo-first-order conditions ($I \geq 5E$) were maintained, which was verified by the independence of the first-order rate constants on the factor Xa concentration. The increase in fluorescence intensity was followed at a single wavelength. Monophasic traces were obtained with inhibitor concentrations of up to 20 μM without significant variations in the ratio of the amplitudes to the enzyme concentrations. This observation suggests functional equivalence of α- and β-factor Xa present in the protease preparation (Figure 4) with respect to the reaction with the inhibitor as well as homogeneity of the inhibitor. The dependence of the observed rate constant on the inhibitor concentration is illustrated in Figure 7.

The hyperbolic increase is consistent with a two-step mechanism, where the bimolecular association of the enzyme and inhibitor is followed by a unimolecular isomerization step (Scheme 2). Since the amplitudes of the fluorescence enhancement do not increase with the concentration of inhibitor, the single optical transition diagnosed by SVD analysis cannot occur at the transition of E + I → EI, but has to be linked to the unimolecular step. The analysis of the stopped flow data makes it possible to assign rate constants to some of the reaction steps illustrated in Scheme 2. The *y*-intercept of approximately zero obtained for the saturation function of k_{obs} with increasing C921-78 concentrations is incompatible with the rapid equilibrium assumption ($k_1 I$, $k_2 \gg k_3$) (*30*, *39*) since it requires either or both k_2 and k_4 to be $<10^{-2}$ s^{-1}. This is further supported by the ratio

of the midpoint $K_{0.5}$ to the slope of the initial portion of the hyperbola, which limits k_2 to ~100 s^{-1}. Thus, the initial slope of the hyperbola yields an upper estimate for the bimolecular rate constant for the formation of the EI complex of 5.3×10^{-6} M^{-1} s^{-1}, which is in agreement with the rate constant determined in inhibition studies. The limiting value of $k_{obs}t$ at saturating inhibitor concentrations yields a value for $k_3 + k_4$ of 142 s^{-1} for the subsequent isomerization step (Scheme 2). The uncertainty in the value of the *y*-intercept does not permit an assessment of k_2 and k_4 from the present data. However, in agreement with previous mechanistic studies on the reaction of protease with tight inhibitors, the slow dissociation of C921-78 from factor Xa demonstrated in steady state studies was attributed to the reversal of the isomerization step. Consequently, k_4 was assigned a value of $\sim 1 \times 10^{-4}$ s^{-1}, and the limiting value of k_2 was ~100 s^{-1}. Numerical simulations of progress curves for the reaction of C921-78 with factor Xa using the assigned values for the rate constants of the reaction steps yielded a highly similar dependence of k_{obs} on the concentration of C921-78.

The rapid kinetic studies demonstrate a two-step mechanism for the reaction of C921-78 with factor Xa, involving a conformational change after a bimolecular association step. The high stability of the complex might result from the rapid rate of the second step and the very slow rate for the reversal of the reaction, characterized by k_2 and k_4.

DISCUSSION

In the work presented here, $BnSO_2$-Arg-Gly-Arg-ketothiazole (C921-78) was found to be a selective and tight inhibitor of human factor Xa. Kinetic studies on the inhibition of substrate hydrolysis by C921-78 indicate reversible, competitive binding to factor Xa. With a dissociation constant of 14 pM, it can be considered one of the most potent small molecule inhibitors for serine proteases described so far. The formation of the C921-78−factor Xa complex results in a fluorescence enhancement, which was used to monitor the reaction of the enzyme and inhibitor in a stopped flow fluorometer. The results related the fluorescence increase to the unimolecular isomerization, which occurs after the bimolecular formation of the complex. The kinetic constant for the bimolecular step obtained by fluorescence measurements is consistent with that obtained for the slow onset of enzyme inhibition, thereby linking both processes to the same molecular event. The rate constants for the two steps of complex formation are inconsistent with the assumption of rapid equilibrium for the initial step of the reaction in contrast to the classical mechanism formulated for inhibition in two steps. Thus, the overall mechanism of the inhibition of factor Xa by C921-78 supports recent evidence for deviations from the classical mechanism for slow tight binding inhibition, where an initial inhibitor−enzyme complex (EI) forms in a rapid preequilibrium to the slow rearrangement to EI**.

The primary structure of C921-78 is closely related to the Lys-Gly-Arg sequence of the autolysis loop of factor Xa. The published model of Brandstetter et al. (*40*) of this region bound to the active site of factor Xa allows conclusions about the position of the peptide portion of the inhibitor in the active site to be drawn. Large contributions to the binding energy may result from the formation of a salt bridge between the C-terminal Arg and Asp189 in the specificity pocket. The accommodation of the inhibitor in the active site is facilitated by the small Gly residue, since it reduces the strength of unfavorable interactions in the sterically restricted S2[3] site of factor Xa. The preference of factor Xa for Gly in this position is further corroborated by the fact that it is found at the homologous position in natural factor Xa ligands, prothrombin and antithrombin III, as well as in the best synthetic substrates S-2222 and S-2765 (*41*). Accordingly, Gly may destabilize the interaction with activated protein C and thrombin, which both prefer the voluminous and rigid Pro in P2. Thus, Gly in P2 appears to be pivotal for the specificity of C921-78 for factor Xa (*40*, *41*). In contrast, the contribution of D-Arg at P3 of the inhibitor has to remain undetermined, as the homologous Lys of the autolysis loop appears to be completely solvent-exposed. In addition, favorable electrostatic interactions appear to be unlikely to contribute to the stability of the complex, since several ligands of factor Xa have a Glu at this position. Comparison with the sterically similar bisamidino compounds suggests a potential interaction with a putative P4 pocket by cation π interactions (*42*, *43*). The high degree of complementarity between C921-78 and the substrate recognition site of factor Xa may also produce enough latent binding energy to facilitate conformational changes required for the transition state like binding of the ketothiazole group to Ser195 and His57. The efficient formation of the transition state analogue is suggested by the calculation of the binding energy, which is 90% of that calculated for the transition state intermediate of peptide hydrolysis (*15*). A similar enhancement in the reactivity of the catalytic triad with substrates or transition state inhibitors by favorable interactions of the ligand in P1−P3 was observed for chymotrypsin and elastase (*15*, *17*, *44*).

A critical role for thiazole in the binding of the inhibitor suggests the selectivity of C921-78 for factor Xa versus trypsin, which is inconsistent with the almost identical K_m of these enzymes for S-2765 [38 and 28 μM for factor Xa and trypsin, respectively (unpublished results)]. X-ray structures of a peptide α-ketothiazole with thrombin suggest a contribution from the interactions of the heterocycle with a putative S1′ site, which modulates the affinity of the compound for the enzyme. As the thiazole binds weakly if at all to factor Xa ($K_d \sim 1$ M^{-1}, $\Delta G = 0$ kJ mol^{-1}) and a micromolar dissociation constant for the peptide component can be assumed (from the K_m of the substrate S-2765), the high affinity of C921-78 cannot result from the sum of the binding energies of the components alone. The difference may be attributed to the smaller loss of translational entropy that is necessary for the accommodation of the thiazole in sites of factor Xa, when it is joined covalently to the peptide. This entropic advantage results from the conversion of the reaction of the thiazole with factor Xa from a bimolecular to an intramolecular process as a consequence of the initial binding of the peptide chain. An estimate for the significance of this effect provides the ratio of the rate constants for the transition of EI to EI*, which indicates 300000-fold more favorable binding of the thiazole in C921-78 than can be expected when it reacts independently with factor Xa. Thus, the high affinity and selectivity of C921-78 for factor Xa are derived from highly favorable interactions in S1−S3 and

[3] Nomenclature of Schechter and Berger (*2*).

at a putative S1′ site, amplified by an advantageous entropy effect comparable to that of chelating agents to polyvalent cations.

In previous studies, the reaction of α-ketothiazole with elastase, thrombin, and prolyl endopeptidase was found to occur without a detectable delay on the time scale of the assays (*11*, *48*, *49*). In contrast, C921-78 inhibits the hydrolytic activity of factor Xa with a slow onset. The slow equilibration of the enzyme and inhibitor may result from a slow transition of the enzyme or inhibitor to the reactive form or the slow isomerization of an initial enzyme−inhibitor complex. The dependence of k_{inh} on the inhibitor concentration excludes a hysteretic behavior of the enzyme. The alternative possibility of slow conversion of a hydrated nonreactive form of the inhibitor to a reactive one could be excluded with some certainty by the results of NMR studies on analogous α-ketothiazole inhibitors (*48*). The fluorescence stopped flow studies, however, provide evidence for the formation of the enzyme−inhibitor complex occurring in two steps.

For the classical interpretation of the kinetics of slow tight binding inhibition, the enzyme−inhibitor complex is assumed to be in rapid equilibrium with the components ($k_1I \gg k_3$ and $k_2 \gg k_3$). Since with $k_1I \leq k_3$ and the upper limit of $k_2 \sim k_3$ the steps (Scheme 2) cannot be separated kinetically, the reaction is more appropriately described by a steady state formalism. Two boundary conditions apply, depending on the ratio of k_3/k_2 (*51*). If $k_3 \gg k_2$, the association rate constant is reduced to k_1 and k_{obs} increases linearly with the concentration of inhibitor. In contrast, when $k_2 \approx k_3$, there is a hyperbolic dependence of k_{obs} on increasing inhibitor concentration. The present data appear to be consistent with the latter case, therefore justifying the assignment of 100 s^{-1} for k_2. With these estimates for the rate constants of the steps in the formation of the C921-78−factor Xa complex, a K_{init} of 100 μM for the dissociation constant of EI (Scheme 2) was obtained using the expression $K_{init} = k_3(1 + k_2/k_1)/k_1$ (*52*). This similarity of the K_{init} values of C921-78 and the K_m values of S-2765 suggests that the initial binding of I to E is adequately approximated by the binding of the homologous peptide. The ratio of k_4/k_3 indicates a 300000-fold enhancement in the stability resulting from the unimolecular isomerization. The rapid rate indicates an extremely favorable conformational change leading to the effectively irreversible inhibitor−factor Xa complex (EI*). This gain in stability is comparable to that attributed to the interaction of antithrombin III with the Ser195 of thrombin resulting in formation of the tetrahedral adduct (*50*) and the formation of the hemiketal by reaction of Ser195 with trifluoromethyl ketones in studies with elastase (*15*). Thus, the increase in fluorescence is potentially related to the conformational changes associated with the formation of the hemiketal by reaction of Ser195 with the α-ketothiazole portion of C921-78.

The magnitude of the observed fluorescence change is consistent with a decrease in the extent of solvent exposure of fluorescence residues, in particular Trp. Of the four Trp residues in the heavy chain of factor Xa, only Trp215 is located close to the active site. The conformational change accompanying the transition from EI to EI* may involve repositioning of the inhibitor moiety, which causes a change in fluorescence by altering the interaction Trp215 and the Arg residues of C921-78. Alternatively, the fluorescence changes induced by occupation of the active site by C921-78 may not be due to a direct interaction of the inhibitor with a fluorophore, but may result from conformational changes in the protease. For example, the fluorescence changes induced by the binding of active site ligands to thrombin are related to a structural reorganization of regions within 60 Å of the region occupied by the ligand (*38*). In either case, formation of the stable inhibitor−enzyme complex EI* is associated with conformational perturbations of the enzyme, inhibitor, or both, in contrast to the "lock and key" mechanism determined from X-ray structures of related inhibitor to protease. The alternative mechanisms of the binding of C921-78 to factor Xa, however, cannot be resolved with the present data.

The procoagulant activity of factor Xa requires its incorporation into prothrombinase, which increases the efficiency of prothrombin cleavage 300000-fold (*4*). Consequently, prothrombinase is considered the relevant catalyst for thrombin formation, and the affinity of C921-78 for prothrombinase is an important consideration for evaluating the anticoagulant potential. In the study presented here, however, the dissociation constants of C921-78 with factor Xa and prothrombinase were found to be equivalent. Accordingly, the interaction of factor Xa and factor Va is without effect on the recognition sites of the protease for C921-78 and the active site residues, which are tethered to the inhibitor by Ser195 and His57. This lack of an effect of the cofactor on the binding of inhibitor confirms earlier kinetic studies on the covalent modification of His57 and Ser195 by DEGR-CMK (*28*). These observations, however, are inconsistent with the past explanations for the higher efficiency of prothrombin cleavage by prothrombinase relative to that by factor Xa by assuming differences in the catalytic site (*45*). In contrast, they provide circumstantial evidence for cofactor-induced alterations at sites far from the active site, which facilitate the binding of the macromolecular ligands (*46*, *47*).

The formation of the inhibitory complex is characterized by unusually favorable energetics of the formation of EI*, which will result in a long lifetime for the factor Xa−C921-78 complex under physiologic conditions. Because of its high inhibitory potency and selectivity versus related coagulation proteases, C921-78 has potential as an anticoagulant.

ACKNOWLEDGMENT

We thank Dr. S. Krishnaswamy for the critical review of the manuscript.

REFERENCES

1. Bode, W., Mayer, I., Baumann, U., Huber, R., Stone, S. R., and Hofsteenge, J. (1989) *EMBO J. 11*, 3467−3475.
2. Schechter, I., and Berger, A. (1967) *Biochem. Biophys. Res. Commun. 27*, 157−162.
3. Mann, K. G., Jenny, R. J., and Krishnaswamy, S. (1988) *Annu. Rev. Biochem. 57*, 915−956.
4. Mann, K. G., Nesheim, M. E., Church, W. R., Haley, P., and Krishnaswamy, S. (1990) *Blood 76*, 1−16.
5. Kalafatis, M., Swords, N. A., Rand, M. D., and Mann, K. G. (1994) *Biochim. Biophys. Acta 994*, 113−129.
6. Broze, G. J. (1995) *Annu. Rev. Med. 46*, 103−112.
7. Scully, M. F. (1992) *Semin. Thromb. Hemostasis 18*, 218−223.
8. Vlasuk, G. P. (1993) *Thromb. Haemostasis 70*, 212−216.

9. Dunwiddie, C., Thornberry, N. A., Bull, H. G., Sardana, M., Friedman, P., John, W. J., and Simpson, E. (1989) *J. Biol. Chem. 264*, 16694−16699.
10. Scarborough, R. M. (1998) *J. Enzyme Inhib. 14*, 15−25.
11. Edwards, P. D., Meyer, E. F., Vijayalakshmi, J., Tuthill, P. A., Andisk, D. A., Gomes, B., and Strimpler, A. (1992) *J. Am. Chem. Soc. 114*, 1854−1863.
12. Matthews, J. H., Krishnan, R., Costanzo, M. J., Maryanoff, B. E., and Tulinsky, A. (1996) *Biophys. J. 71*, 2830−2839.
13. Poulos, T. L., Alden, R. A., Freer, S. T., Birktoft, J. J., and Kraut, J. (1976) *J. Biol. Chem. 251*, 1097−1103.
14. Imperiali, B., and Abeles, R. H. (1986) *Biochemistry 25*, 3760−3767.
15. Brady, K., and Abeles, R. H. (1990) *Biochemistry 29*, 7608−7617.
16. Bonneau, P., Grand-Maitre, C., Greenwood, D. J., Lagace, L., LaPlante, S. R., Massariol, M.-J., Ogilvie, W. W., O'Meara, J. A., and Kawai, S. (1997) *Biochemistry 36*, 12644−12652.
17. Stein, R. L., and Strimpler, A. M. (1987) *Biochemistry 26*, 2611−2615.
18. Nilsson, T., Sjoling-Ericksson, A., and Deinum, J. (1998) *J. Enzyme Inhib. 13*, 12−29.
19. Edwards, P. D., Wolanin, D. J., Andisik, D. W., and Davis, M. W. (1995) *J. Med. Chem. 38*, 76−85.
20. Lottenberg, R., and Jackson, C. M. (1983) *Biochim. Biophys. Acta 874*, 326−336.
21. MacDonald, R. C., MacDonald, R. I., Menco, B. P., Takeshita, K., Subbarao, N. K., and Hu, L. R. (1991) *Biochim. Biophys. Acta 1061*, 297−303.
22. Gomori, G. (1942) *J. Lab. Clin. Med. 27*, 955−960.
23. Nesheim, M. E., Eid, S., and Mann, K. G. (1984) *J. Biol. Chem. 256*, 9874−9882.
24. DiScipio, R. G., Hermodson, M. A., Yates, S. G., and Davie, E. W. (1977) *Biochemistry 16*, 698−707.
25. Fenton, J. W., Fasco, M. J., Stackrow, A. B., Aronson, D. L., Young, A. M., and Finlayson, J. S. (1977) *J. Biol. Chem. 252*, 3587−3598.
26. Fasman, G. D. (1975) *Handbook of Biochemistry and Molecular Biology*, 3rd ed., Vol. II, CRC Press, Cleveland, OH.
27. Selwyn, M. J. (1965) *Biochim. Biophys. Acta 105*, 193−195.
28. Walker, R. K., and Krishnaswamy, S. (1993) *J. Biol. Chem. 268*, 13920−13929.
29. Bevington, P. R. (1969) *Data Reduction and Error Analysis in the Physical Sciences*, McGraw Hill, New York.
30. Segel, I. H. (1975) *Enzyme Kinetics. Behavior and Analysis of Rapid Equilibrium and Steady State Enzyme Systems*, John Wiley & Sons, New York.
31. Leytus, S. P., Toledo, D. L., and Mangel, W. F. (1984) *Biochim. Biophys. Acta 788*, 74−86.
32. Morrison, J. F., and Walsh, C. T. (1988) *Adv. Enzymol. 61*, 437−467.
33. Williams, J. W., Morrison, J. F., and Duggleby, R. G. (1979) *Biochemistry 18*, 2567−2563.
34. Cha, S. (1975) *Biochem. Pharmacol. 24*, 2177−2185.
35. Hofsteenge, J., and Stone, S. R. (1986) *Biochemistry 25*, 4622−4628.
36. Hendler, R. W., and Shrager, R. I. (1994) *J. Biochem. Biophys. Methods 28*, 1−33.
37. Kettner, C., and Shaw, E. (1981) *Thromb. Res. 22*, 645−652.
38. Parry, M. A., Stone, S. R., Hofsteenge, J., and Jackman, M. P. (1993) *Biochem. J. 290*, 663−670.
39. Fromm, H. J. (1975) *Initial Rate Steady State Kinetics*, Springer Verlag, Berlin and New York.
40. Brandstetter, H., Kühne, A., Bode, W., Huber, R., Saal, W. v. d., Wirthensohn, K., and Engh, R. A. (1996) *J. Biol. Chem. 271*, 29988−29992.
41. Lottenberg, R., Hall, J. A., Pautler, E., Zupan, A., Christensen, U., and Jackson, C. M. (1986) *Biochim. Biophys. Acta 874*, 326−336.
42. Lin, Z., and Johnson, M. E. (1995) *FEBS Lett. 370*, 1−5.
43. Maduskuie, T. P., McNamara, K. J., Ru, Y., Knabb, R. M., and Stouten, P. F. W. (1998) *J. Med. Chem. 41*, 53−62.
44. Thompson, R. C., and Bauer, C.-A. (1979) *Biochemistry 18*, 1552−1559.
45. Rezaie, A. R., and Esmon, C. T. (1995) *J. Biol. Chem. 270*, 16176−16181.
46. Krishnaswamy, S., and Walker, R. K. (1997) *Biochemistry 36*, 3319−3330.
47. Betz, A., Vlasuk, G. P., Bergum, P. W., and Krishnaswamy, S. (1997) *Biochemistry 36*, 181−191.
48. Tsutsumi, T., Okonogi, T., Shibahara, S., Ohuchi, S., Hatsushiba, E., Patchett, A. A., and Christensen, B. G. (1994) *J. Med. Chem. 37*, 3492−3502.
49. Constanzo, M. M., Maryanoff, E. B., Hecker, L. R., Schott, R. M., Yabut, C., Zhang, C. H., Andrade-Gordon, P., Kauffman, J. A., Lewis, J. M., Krishnan, R., and Tulinski, A. (1996) *J. Med. Chem. 39*, 3039−3043.
50. Stone, S. R., and Bonniec, B. L. (1997) *J. Mol. Biol. 265*, 344−362.
51. Sculley, M. J., Morrison, J. F., and Cleland, W. W. (1996) *Biochim. Biophys. Acta 1298*, 78−86.
52. Stone, S. R., and Hermans, J. M. (1995) *Biochemistry 34*, 5164−5172.
53. Lewis, S. D., Lucas, B. J., Brady, S. F., Sisko, J. T., Cutrona, K. J., Sanderson, P. E., Freidinger, R. M., Mao, S. S., Gardell, S. J., and Shafer, J. A. (1998) *J. Biol. Chem. 273*, 4843−4845.

BI990958A